Environmental Science & Technology

pubs.acs.org/est

Article

De Novo Development of a Quantitative Adverse Outcome Pathway (qAOP) Network for Ultraviolet B (UVB) Radiation Using Targeted Laboratory Tests and Automated Data Mining

You Song,* Li Xie, YeonKyeong Lee, and Knut Erik Tollefsen*

Cite This: https://dx.doi.org/10.1021/acs.est.0c03794

Read Online

ACCESS | Metrics & More | Article Recommendations | Supporting Information

ABSTRACT: Ultraviolet B (UVB) radiation is a natural nonchemical stressor posing potential hazards to organisms such as planktonic crustaceans. The present study was conducted to revisit the lethal effects of UVB on crustaceans, generate new experimental evidence to fill in knowledge gaps, and develop novel quantitative adverse outcome pathways (qAOPs) for UVB. A combination of laboratory and computational approaches was deployed to achieve the goals. For targeted laboratory tests, *Daphnia magna* was used as a prototype and exposed to a gradient of artificial UVB. Targeted bioassays were used to quantify the effects of UVB at multiple levels of biological organization. A toxicity pathway network was assembled based on the new experimental evidence and previously published data extracted using a novel computational tool, the NIVA Risk Assessment Database (NIVA RAdb). A network of AOPs was developed, and weight of evidence was assessed based on a combination of the current and existing data. In addition, quantitative key event relationships in the AOPs were developed by fitting the *D. magna* data to predefined models. A complete workflow for assembly and evaluation of qAOPs has been presented, which may serve as a good example for future de novo qAOP development for chemical and nonchemical stressors.

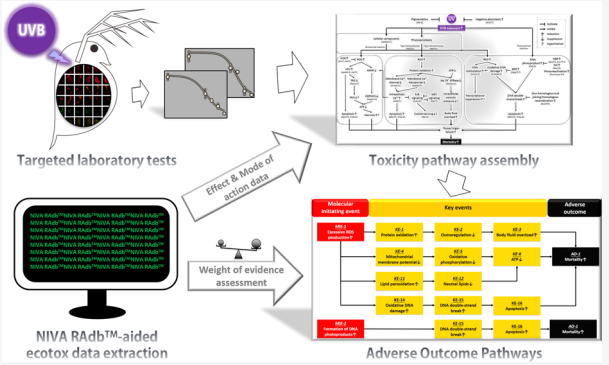

INTRODUCTION

The adverse outcome pathway (AOP) framework has been introduced to better organize (eco)toxicological data relevant for environmental hazard and risk assessment.[1] An AOP causally links the molecular initiating event (MIE) of a stressor with its biological target, a series of key events (KEs) occurring at increasing levels of biological organization, and an adverse outcome (AO) of regulatory concern.[2,3] The confidence and applicability of an AOP can be defined by weight of evidence (WoE) assessment based on Bradford-Hill considerations.[4] An AOP network is an advanced form of AOP, which integrates two or more linear AOPs to better capture the biological complexity in a network of causal relationships.[5,6] With the support from the AOP framework, new approach methodologies (NAMs) such as in vitro high-throughput screening (HTS), toxicogenomics, and computational modeling can be better implemented to refine, reduce, or replace conventional approaches, thus reducing laboratory (eco)toxicity tests and efficiently cover a higher number of environmental stressors to inform Integrated Approaches to testing and Assessment (IATA).[7] However, although more than 300 AOPs have been deposited in the public AOP repository AOPWiki (https://aopwiki.org/), the current AOP framework is heavily chemical-centric, and only a limited number of initiatives (e.g., ref.[1,8−13]) have been made to develop AOPs for nonchemical stressors, such as ionizing radiation, UV, and climate stressors. In a long-term perspective, lack of robust AOPs for nonchemical stressors may limit future applications of the AOP framework toward screening, prioritization, hazard assessment, and even cumulative risk assessment (CRA) of multiple stressors. More efforts to develop AOPs for nonchemicals are therefore highly warranted. In addition, the majority of the AOPs submitted to the AOPWiki lack WoE assessment, possibly due to difficulties to efficiently identify high-quality supporting data. Hence, there is also an urgent need to develop efficient WoE assessment strategies, which can better utilize advanced computational tools for efficient data mining and filtration.

Ultraviolet radiation (UVR) is a natural electromagnetic radiation with wavelengths ranging from 10−400 nm and a common nonchemical stressor to the biota. Major types of solar UVR, such as UVC (100−280 nm), can be completely

Received: June 10, 2020
Revised: August 31, 2020
Accepted: September 14, 2020
Published: September 14, 2020

absorbed by the stratospheric ozone layer. Ultraviolet B (280−315 nm) can be partially absorbed by ozone before reaching the Earth's surface, whereas UVA (315−400 nm) can completely penetrate the atmosphere and reach greater water depths. Nevertheless, UVB is considered more harmful than UVA to living organisms due to its shorter wavelength and higher photon energy. Historical anthropogenic activities have led to decreased stratospheric ozone[14] and increased UVB intensity on the Earth's surface. Although some of the concern expressed for depletion of the ozone layer is reduced, elevated UVB levels may persist for another half century[15] and have negative impacts on the ecosystems.[16]

The effects and modes of action (MoAs) of UVB have been extensively studied. Two initial biochemical reactions are relatively better characterized for UVB and found to be common to a high number of organisms. One is direct damage to DNA through formation of photoproducts such as cyclobutane pyrimidine dimers (CPDs) and pyrimidine 6−4 pyrimidone photoproducts (6-4PPs) (reviewed in a study by Rastogi et al.[17]). The other is induction of oxidative damage to DNA, lipids, and proteins through generation of excessive reactive oxygen species (ROS) (reviewed in a study by Cadet et al.[18]). If not reduced by defensive mechanisms such as photo-protective pigmentation, antioxidant defense, behavioral changes, and DNA repair, the damage may lead to permanent perturbations at different levels of biological organization and subsequently result in adverse effects such as increased mortality, reduced reproduction, growth arrest, developmental abnormalities, altered geographical distribution, and changes to food-web structures.[19] Although the effects of UVB have been extensively documented for a range of organisms, the causality between UVB-induced CPD and ROS formation and regulatory relevant adverse effects has not been fully established.

Zooplankton inhabiting in the water surfaces are usually vulnerable to increased UVB irradiance.[20] The water flea *Daphnia* are among the most susceptible zooplankton species in the freshwater ecosystems and have been widely used as prototypical invertebrate models for studying the impact of UVB.[21−25] The present study therefore used *Daphnia magna* in targeted laboratory tests to fill in knowledge gaps. A novel computational tool, the NIVA Risk Assessment Database (RAdb), was employed for efficient data mining and extraction to support de novo AOP assembly and evaluation. In addition, common model fitting approaches were used to quantify the KERs in the AOP network. The main objectives of the study were to (1) systematically assess the effects of UVB on *D. magna* at multiple levels of biological organization to fill in knowledge gaps; (2) assemble a toxicity pathway network of UVB-mediated lethal effects on *D. magna* based on a combination of new experimental evidence and existing data extracted using the NIVA RAdb; and (3) develop and evaluate a new qAOP network for UVB-mediated lethal effects on crustaceans.

MATERIALS AND METHODS

UV Exposure. The detailed experimental procedures are described in Supporting Information (SI) 1 (Supporting Information-1). In brief, *Daphnia magna* (DHI strain) were cultured in a standard manner according to the OECD test guideline 211.[26] The UV exposures (7 days, light:dark = 16 h:8 h) were conducted in a custom-made UV irradiation chamber equipped with UVA, UVB, and white light tubes to produce a gradient of UVB irradiance (0.0008, 0.05, 0.1, 0.2, and 0.4 W/m^2) combined with a constant UVA irradiance (0.4 W/m^2) and visible light irradiance (20 μmol/m^2·s). The spectrum and dosimetry of UV tubes were measured using a scanning spectroradiometer (Bentham DTM 300, Bentham Instruments Ltd., Reading, UK) and a broadband spectrometer (SpectroSense2+, Skye Instruments Ltd., Llandrindod Wells, UK), respectively. The total exposure doses (kJ/m^2) were calculated as the product of irradiance and time (Supporting Information−2, Table S3). Due to limited space in the exposure chamber, four exposures were conducted sequentially (Supporting Information−2, Table S1) to generate enough materials for testing all endpoints of interest. The majority of the daphnids were sampled after 2 days of exposure for targeted bioassays, whereas the remaining animals were continuously exposed to UVB for 7 days to determine lethal effects. It should also be noted that the exposure setup in this study was specifically designed to trigger toxicity pathways and facilitate qAOP development. Addressing environmentally relevant UVB exposure scenarios and potential adaptive responses in organisms was not the primary goal of this design.

Targeted Bioassays. A suite of bioassays was used to determine the effects of UVB at multiple levels of biological organization in *D. magna*. The detailed assay procedures can be found in Supporting Information−1. In brief, a high-throughput quantitative real-time reverse transcription polymerase chain reaction assay (HT-qPCR, n = 4) was used to determine transcriptional responses of genes known to be or likely involved in UVB-mediated toxicity pathways in *D. magna* after 2 days of exposure, according to the established method.[27,28] Fluorometric measurements of cellular ROS (cROS, n = 3), mitochondrial ROS (mROS, n = 3), and lipid peroxidation (LPO)-associated ROS (lpoROS, n = 3) in *D. magna* after 2 days of exposure were performed using the probes 2′,7′-dichlorodihydrofluorescein diacetate (H_2DCFDA), dihydrorhodamine 123 (DHR123) and 4,4-difluoro-3a,4adiaza-s-indacene (BODIPY), respectively, as previously described.[8,29] 8-Oxo-2′-deoxyguanosine (8-OHdG) was used as a biomarker to indicate oxidative DNA damage in *D. magna* after 2 days of exposure to UVB. The 8-OHdG assay (n = 4) was performed using the fluorometric EpiQuik 8-OHdG DNA Damage Quantification Direct Kit (Epigentek, New York, USA) based on 100 ng purified genomic DNA following the manufacturer's protocol. Protein carbonylation was used as a marker for protein oxidation in *D. magna* after 2 days of exposure. The protein carbonylation assay (n = 5) was performed using the Protein Carbonyl Content Assay Kit (Abcam, Cambridge, UK) according to the producer's instructions. A cyclobutane pyrimidine dimer (CPD) was used as a marker of DNA photoproduct formation in *D. magna* after 2 days of exposure. The CPD assay (n = 4) was performed using the OxiSelect UV-induced DNA Damage ELISA Kit (Cell Biolabs, San Diego, USA) based on 50 ng purified genomic DNA as described in the manufacturer's manual. The tetramethylrhodamine methyl ester perchlorate (TMRM) assay was used to determine the mitochondrial inner membrane potential (MMP) in *D. magna* after 2 days of exposure to UVB, as described elsewhere.[8] The whole-organism ATP content (n = 4) was determined in *D. magna* after 2 days of exposure using the fluorometric ATP Assay Kit (Abcam), according to the manufacturer's protocol. The Nile red assay was used to determine the amount of storage neutral lipid droplets (triacylglycerols) in *D. magna* after 2 days of

https://dx.doi.org/10.1021/acs.est.0c03794
Environ. Sci. Technol. XXXX, XXX, XXX−XXX

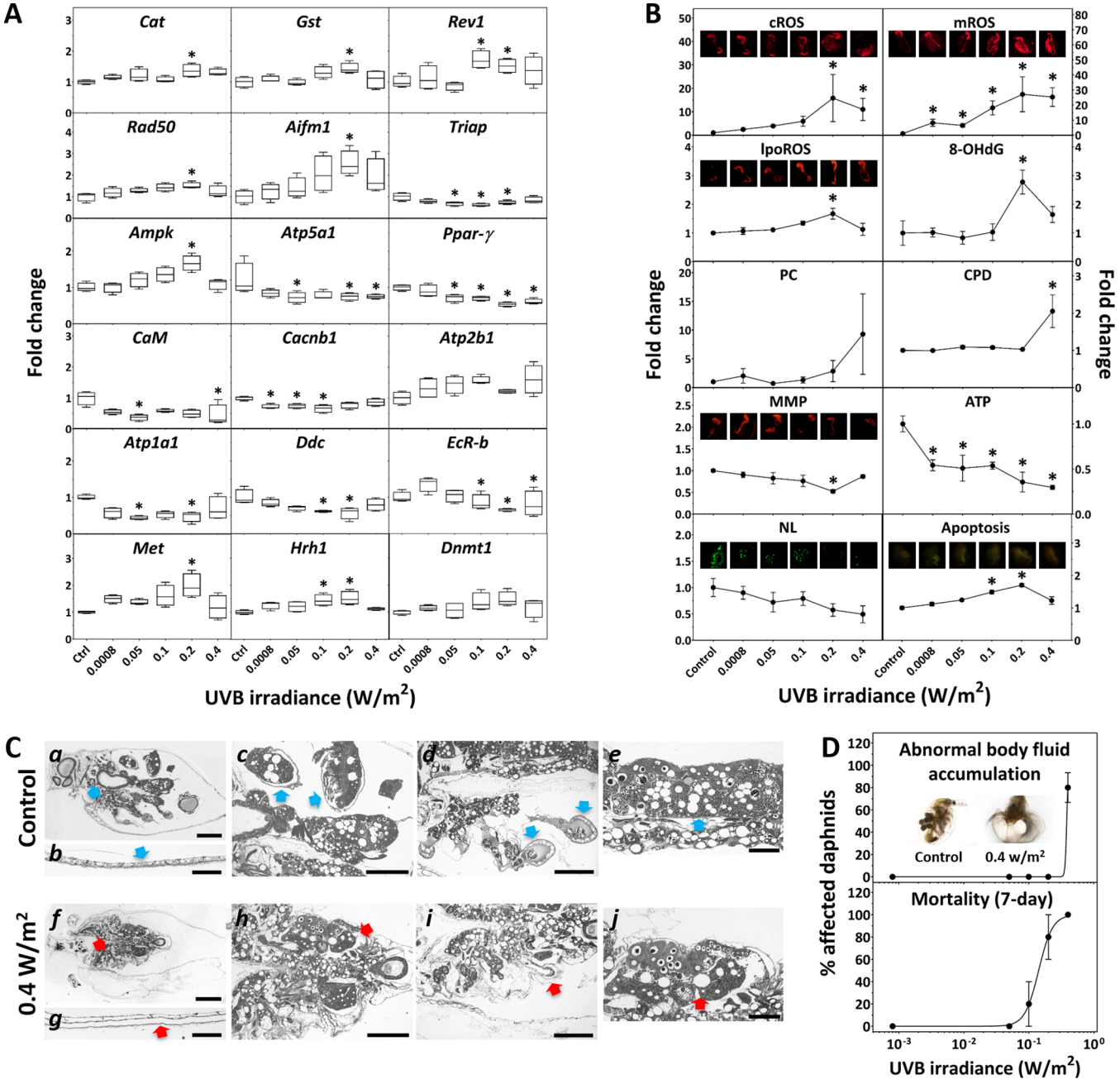

Figure 1. Effects of ultraviolet B (UVB) radiation on *Daphnia magna* after 2−7 days of exposure. (A) Transcriptional responses; (B) cellular responses; (C) tissue/organ responses, (a−e) controls, and (f−j) 0.4 W/m^2 UVB exposed. (a and f) overview of the control and exposed *D. magna*, respectively, (b and g) epidermis in the control and exposed *D. magna*, respectively, (c and h) embryo development in the control and malformation in exposed *D. magna*, respectively, (d and i) thoracopod development in the control and exposed *D. magna*, respectively, and (e and j) ovary development in the control and exposed *D. magna*, respectively. Scale bars: (a and f) 400 μm. (c, d, h, i) 250 μm, and (b, g, e, j) 100 μm. Blue arrows indicate normal tissue/organ structures in the controls; red arrows indicate abnormal tissue/organ structures. (D) Irradiance-response curves of abnormal body fluid accumulation (top) after 2 days of exposure and mortality after 7 days of exposure (bottom). *Cat*: catalase; *Gst*: glutathione s-transferase; *Rev1*: DNA repair protein REV1; *Rad50*: DNA repair protein RAD50; *Aifm1*: apoptosis-inducing factor 1; *Triap*: TP53-regulated inhibitor of apoptosis 1; *Ampk*: 5′-amp-activated protein kinase catalytic subunit alpha; *Atp5a1*: ATP synthase subunit alpha, mitochondrial; *Ppar-γ*: peroxisome proliferator-activated receptor gamma coactivator-related protein; *CaM*: calmodulin; *Cacnb1:* voltage-dependent L-type calcium channel subunit beta-1 protein; *Atp2b1*: plasma membrane calcium-transporting ATPase; *Atp1a1*: sodium/potassium-transporting ATPase subunit alpha; *Ddc*: aromatic-L-amino-acid decarboxylase; *EcR-b*: ecdysone receptor B; *Met*: methoprene-tolerant; *Hrh1*: histamine H1 receptor; *Dnmt1*: DNA (cytosine-5)-methyltransferase 1. cROS: cellular reactive oxygen species (ROS); mROS: mitochondrial ROS; lpoROS: lipid peroxidation associated ROS; 8-OHdG: 8-Oxo-2′-deoxyguanosine; PC: protein carbonylation; CPD: cyclobutane pyrimidine dimers; MMP: mitochondrial inner membrane potential; ATP: adenosine triphosphate; NL: neutral lipids. * denotes significant difference from the control.

exposure, as previously described.[8,30] Whole-organism apoptosis (n = 5) was measured using the terminal deoxynucleotidyl transferase dUTP nick end labeling (TUNEL, Sigma-Aldrich) assay, as previously described.[8] Histopathological

https://dx.doi.org/10.1021/acs.est.0c03794
Environ. Sci. Technol. XXXX, XXX, XXX−XXX

analysis was performed to identify UVB-induced damage to *D. magna* tissues and organs after 2 days of exposure, as previously described.[8] Visual observations were performed daily to record mortality and abnormalities at the individual level. The bioassay data were analyzed in GraphPad Prism v8 (GraphPad Software Inc., San Diego, USA) using common statistical methods such as ANOVA and logistic regression (Supporting Information−1).

Automated Data Mining and Extraction. The NIVA RAdb (www.niva.no/radb) was developed as an in-house database and analytical tool to integrate, filtrate, extract, visualize, and analyze ecotoxicological data from multiple sources (Supporting Information−1, Figure S2) The NIVA RAdb covers ecotoxicological data on both chemical and nonchemical stressors and was therefore employed by the present study to perform automated data mining and extraction to support toxicity pathway assembly and WoE assessment of the AOPs.

qKER Model Construction. Quantitative key event relationship (qKER) models were developed based on the present experimental data using the maximum likelihood estimation (MLE) functions in the Benchmark Dose Analysis Software (BMDS, US EPA, https://www.epa.gov/bmds), as previously suggested.[31] In brief, the current experimental data were fitted to five types of frequentist inference models, exponential, hill, linear, polynomial, and power. The best-fit models were selected based on a combination of visual inspection of model fit, goodness-of-fit, and the Akaike information criterion (AIC).[32]

AOP Assembly and WoE Assessment. Conceptual AOPs were assembled according to OECD's AOP handbook.[33] The WoE assessment was performed based on the Bradford Hill Considerations.[4] Supporting evidence from a combination of the current experimental evidence and relevant data extracted by the NIVA RAdb was used to assist WoE assessment. The confidence levels of the KEs and KERs are scored as "High", "Moderate", or "Low", following OECD's AOP handbook.[33] The applicability domains (taxa and stressors) of the AOPs were also defined based on relevant data extraction from the NIVA RAdb.

RESULTS AND DISCUSSION

Exposure Quality. The pH in the exposure media was 8.0 ± 0.2 and dissolved oxygen higher than 7 mg/L throughout the exposure. The UV dosimetry (Supporting Information −2, Table S3) showed that the measured UVB irradiance was similar to the nominal values (less than 25% deviation) and the UVA irradiance (4.7 ± 0.2 W/m^2, mean ± SD) was stable throughout the exposure.

Effects of UVB on *D. magna*. *Oxidative stress*. After 2 days of exposure, two genes encoding for major antioxidant enzymes catalase (*Cat*) and glutathione *S*-transferase (*Gst*)[34] were upregulated (Figure 1A), indicating elevated demands for producing antioxidants against oxidative stress. Irradiance-dependent increases in ROS from 0 to 0.2 W/m^2 UVB were observed by using multiple types of fluorescent probes (Figure 1B), suggesting cell-wide excessive ROS production and oxidative stress in *D. magna* after 2 days of exposure. Interestingly, a slight decrease in ROS (as well as for many other endpoints in this study) was observed after exposure to 0.4 W/m^2 UVB using the three probes. The mechanistic explanation for this non-monotonic response is not clear. However, it can be speculated that at 0.4 W/m^2, a switch from adaptive/stress responses to death mechanisms occurred after 48 h (albeit no mortality was observed yet), thus making the sublethal endpoints such as ROS and other endpoints not responding monotonically as one would normally expect. UVB-induced oxidative stress has been well documented in *Daphnia* and other crustaceans. Acute (6 h) exposure to 0.14 W/m^2 UVB (total dose: 3.024 kJ/m^2) caused a significant increase in glutathione *S*-transferase (GST) enzymatic activity in adult *D. magna*.[35] Repeated exposure to 8 W/m^2 UVB for 5 h every day during a 12-day period (total dose: 215.28 kJ/m^2) led to significant induction of antioxidant enzymes such as superoxide dismutase (SOD), CAT, GST, and glutathione peroxidase (GPx) in adult *D. magna*.[36] Significant induction of cellular ROS was observed in the adults of the marine copepod *Paracyclopina nana* after 1 h of exposure to 1−4 kJ/m^2 total doses of UVB.[37] Another study on the marine copepod *Tigriopus japonicus* also reported significant increases in ROS formation after 24 h of exposure to total doses of 12 and 24 kJ/m^2 UVB.[38] Although the irradiances were not directly comparable due to the different exposure setup, the total doses used these studies were comparable to those used in the present study (0.1−79.1 kJ/m^2 for 2 days, 0.5−277 kJ/m^2 for 7 days), suggesting that induction of ROS is a common biochemical event in different crustaceans after exposure to UVB. Excessive ROS production is well-known to cause oxidative damage to DNA, proteins, and lipids in organisms.

DNA Damage and Apoptosis. Exposure to UVB is known to cause DNA damage through direct induction of DNA photoproducts or via ROS-mediated oxidative damage (e.g., 8-OHdG) as an indirect effect (reviewed in ref.[39]). It has been reported that the ratio between UVB-induced CPD and 8-OHdG was approximately 100:1 per unit DNA in mammalian cells,[40] suggesting that the formation of photoproducts is likely the major cause of UVB-induced DNA damage in mammals. In the present study, both types of DNA damage were observed in *D. magna* after 2 days of exposure (Figure 1B), with CPD being significantly induced at the highest UVB irradiance (0.4 W/m^2) and the peak 8-OHdG induction observed at a lower irradiance (0.2 W/m^2). In addition, *Rev1*, a gene involved in trans-lesion bypass as a repair mechanism against DNA photoproducts,[41] was also upregulated by exposure to 0.1 and 0.2 W/m^2 UVB (Figure 1A), further supporting the induction of CPD in *D. magna* by UVB. Upregulation of *Rev1* was also found in the copepod *T. japonicus* after 6−48 h exposure to 12 kJ/m^2 UV-B.[42] As only relative measurement of CPD was conducted, it was not possible to calculate the CPD/8-OHdG ratio for *D. magna* in this study. Formation of the DNA photoproduct 6-4PP has been documented for *D. magna* after exposure to 8 W/m^2 UVB for 5 h every day during a 12-day (total dose: 215.28 kJ/m^2) period.[36] Another study has reported formation of CPD in four other *Daphnia* species, including *D. middendorffiana*, *D. pulex*, *D. pulicaria*, and *D. parvula*, after 24 h of exposure to 2.3−9.3 kJ/m^2 UVB.[43] These results collectively support the present finding of increased CPD formation in *D. magna* after UVB exposure. UVB-induced oxidative damage to DNA such as 8-OHdG has not been well studied in crustaceans. However, a study on the marine copepod *T. japonicus* reported significant upregulation of 8-oxoguanine glycosylase (*Ogg1*), a gene responsible for base excision repair (BER) of 8-OHdG, after 12 h of exposure to as low as 10 kJ/m^2 UVB,[44] indicating potential induction of 8-OHdG.

https://dx.doi.org/10.1021/acs.est.0c03794
Environ. Sci. Technol. XXXX, XXX, XXX−XXX

Both DNA photoproduct formation and oxidative DNA damage can lead to DNA double-strand breaks (DSB) (reviewed in ref.[17]). Although no direct measurement of DSB was performed in this study, the irradiance-dependent upregulation of *Rad50* (Figure 1A), a widely used biomarker gene involved in nonhomologous end joining (NHEJ) and homologous recombination (HR) repair of DSB,[45] indicates induction of DNA DSB in *D. magna*. A microarray analysis has also reported significant upregulation of multiple genes involved in NHEJ and HR repair of DNA DSB in *T. japonicus* after 6−48 h of exposure to 12 kJ/m^2 UVB,[42] supporting DNA DSB as a key downstream event of UVB exposure in crustaceans.

It is well known that DNA DSB can activate apoptosis to eliminate damaged cells.[46] Direct measurement using the TUNEL assay showed significant induction of apoptosis in *D. magna* after exposure to 0.1 and 0.2 W/m^2 UVB (Figure 1B). Significant upregulation of the apoptosis initiator *Aifm1*[47,48] by 0.2 W/m^2 UVB and downregulation of the apoptosis inhibitor *Triap*[49] by 0.05−0.2 W/m^2 UVB (Figure 1A) also support elevated apoptotic signaling. The association between UVB exposure and apoptosis has not been well studied in *Daphnia*. However, a study on the swamp ghost crab *Ucides cordatus* showed clear induction of the caspase 3 protein as an indicator of apoptosis after 5 days of exposure to 8.28 kJ/m^2 UVB (irradiance: 11.95 W/m^2, daily irradiation of 23 min for 5 days).[50] By using a combination of TUNEL assay and qPCR, Schramm and coworkers have identified an significant increase in the number of apoptotic cells accompanied by upregulation of genes involved in the apoptotic pathway, such as the tumor antigen *P53*, apoptosis regulator *Bax*, B-cell lymphoma 2 (*Bcl2*), and caspase 3 in the freshwater prawn *Macrobrachium olfersii* after 12 h of exposure to 5.58 kJ/m^2 (irradiance: 3100 W/m^2 for 30 min).[51] Excessive apoptotic death is considered a major contributor to organ dysfunctions and mortality in *D. magna* after exposure to UVB.

Lipid and Energy Metabolism. In the present study, an irradiance-dependent increase in LPO-related ROS was identified (Figure 1B), indicating potential induction of LPO in *D. magna*. UVB-induced LPO has been documented in *D. magna* after repeated exposures to 8 W/m^2 UVB for 5 h every day in a 12-day (total dose: 215.28 kJ/m^2) test period.[36] Acute exposure to 1−4 kJ/m^2 total doses of UVB also led to significant induction of LPO in *P. nana* adults.[37] A direct consequence of LPO is degradation of neutral lipids such as polyunsaturated fatty acids (PUFAs), which are involved in important physiological processes.[52] The apparent irradiance-dependent (albeit nonsignificant) decrease in storage neutral lipid droplets in the present study (Figure 1B) also suggests that exposure to UVB may cause depletion of neutral lipids in *D. magna*. Neutral lipids are key components of the plasma membrane and a major source of cellular energy production.[53,54] It has been reported that exposure to as low irradiance as 0.03 W/m^2 UVB for 2.5−4 h (total dose: 0.285−0.4 kJ/m^2) led to significant reduction in the total lipid content in *D. magna*.[55] As lipid-oriented energy production is highly dependent on neutral lipid metabolism such as fatty acid oxidation (FAO),[53] depletion of neutral lipids may lead to both reduced FAO and subsequent ATP depletion.[56] The present transcriptional analysis further showed that *Ppar-γ*, a nuclear receptor known to positively regulate fatty acid storage,[57] was downregulated in an irradiance-dependent manner (Figure 1A), indicating higher demand for energy metabolism than storage. Decreased fatty acid composition has been associated with acute exposure (48 h) to 1−3 kJ/m^2 UVB in adult female *P. nana*,[37] thus providing additional evidence from a marine crustacean that UVB can affect neutral lipid metabolism. Although lacking direct evidence from crustaceans, the attenuated fatty acid *β*-oxidation pathway has been reported in skin biopsies of SKH-1 mice after chronic exposure to 1.5 kJ/m^2 of UVB three times per week for 30 weeks,[58] supporting FAO reduction as an important downstream event of UVB exposure.

Multiple lines of evidence from the present study also suggest that the mitochondrial ATP production was affected by exposure to UVB. In addition to significant reduction in the mitochondrial MMP at 0.2 W/m^2 (Figure 1B), the gene encoding for ATP synthase subunit *α*, *Atp5a1* was also significantly downregulated by exposure to 0.05, 0.2, and 0.4 W/m^2 UVB (Figure 1A). These results collectively indicate that the activity of mitochondrial OXPHOS was suppressed by UVB. It has been widely recognized that OXPHOS is key for ATP synthesis and cellular energy homeostasis.[59] Direct measurement of the whole-organism ATP content in the present study further supported significant ATP depletion by exposure to as low as 0.0008 W/m^2 UVB (Figure 1B). In addition, the master sensor of cellular energetic status, *Ampk*,[60] was also upregulated by exposure to 0.2 W/m^2 UVB (Figure 1A), indicating cell-wide energy shortage. The effects of UVB on mitochondrial energetic functions have not been well investigated in crustaceans, albeit a study on the freshwater prawn *Macrobrachium olfersi* reported dramatic morphological changes in the mitochondria, such as disrupted outer and inner membranes, mitochondrial fission, and reduction in the number of mitochondrial crests after 30 min of exposure to a high level (irradiance: 3100 W/m^2, total dose: 5.58 kJ/m^2) of UVB.[61] ATP depletion is known to also affect ATP-dependent processes such as membrane ion transport[62,63] and trigger necrotic cell death,[64] which may contribute to organ dysfunctions and mortality in *D. magna* after exposure to UVB.

Protein Oxidation and Ion Regulation. In the present study, an apparent (albeit nonsignificant) increase in the whole-organism protein carbonyl content was observed (Figure 1B), indicating that protein oxidation was likely occurring in *D. magna* after exposure to UVB. UVB-induced protein oxidation has been previously documented in adult *D. magna* after repeated exposure to 8 W/m^2 UVB for 5 h every day during a 12-day (total dose: 215.28 kJ/m^2) test period.[36]

Protein oxidation can lead to malfunctions of key regulators of ion exchange across the plasma membranes.[65,66] The present transcriptional analysis showed that the intracellular calcium sensor *CaM*[67] and the voltage-gated calcium channel *Cacnb1*[68] were downregulated after exposure to UVB, whereas the plasma calcium transporter *Atp2b1*[69] was marginally upregulated (Figure 1A). These findings collectively suggest reduced calcium signaling due to lower intracellular calcium influx (*CaM* and *Cacnb1*) and higher cellular calcium excretion (*Atp2b1*). Calcium plays an important role in various biological processes such as cellular signal transduction, maintenance of membrane potential, and regulation of ion exchange. Influx of intracellular calcium can among others cause mitochondrial dysfunction[70] and trigger apoptosis.[71]

Another important ion regulator for maintaining cellular osmolarity, *Atp1a1*,[72] was significantly downregulated by exposure to 0.05 and 0.2 W/m^2 UVB (Figure 1A), possibly indicating abnormal Na^+/K^+ exchange and osmoregulation in

https://dx.doi.org/10.1021/acs.est.0c03794
Environ. Sci. Technol. XXXX, XXX, XXX−XXX

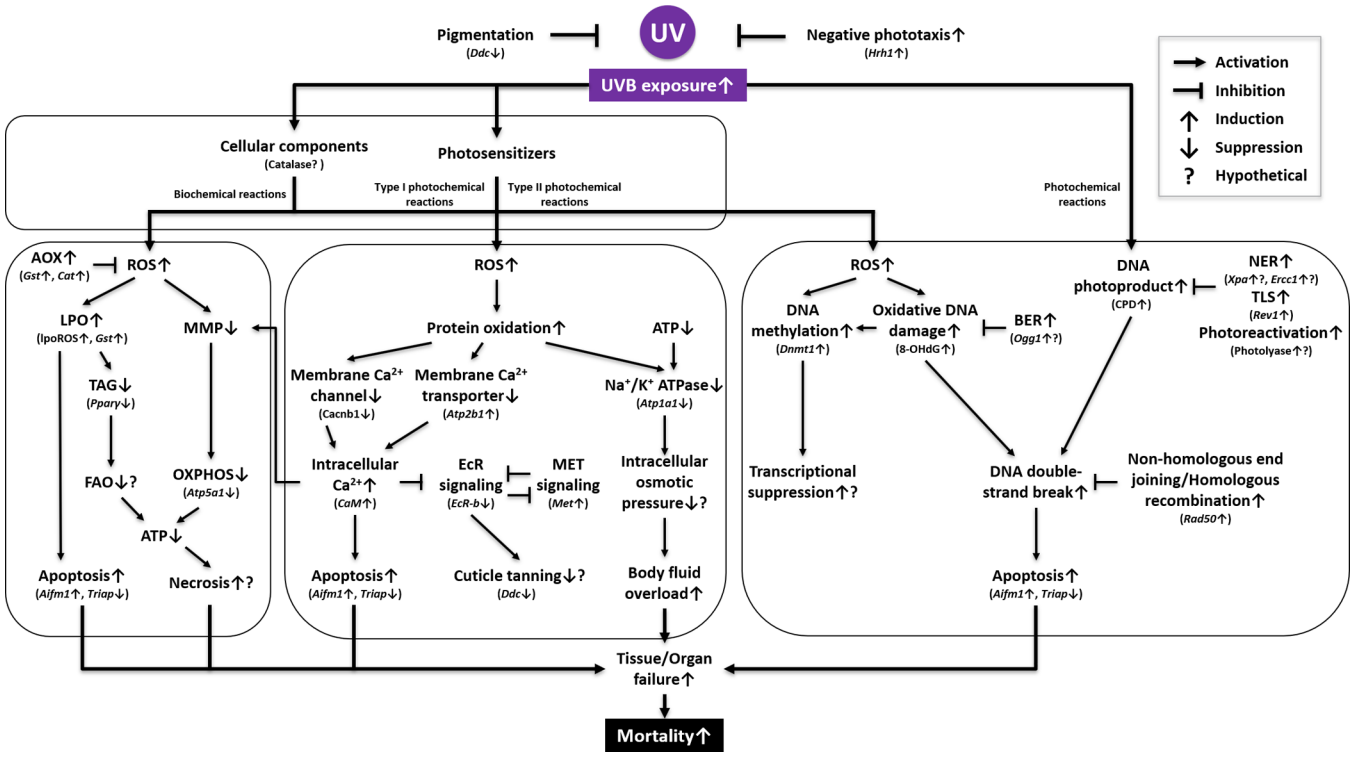

Figure 2. A putative toxicity pathway network of ultraviolet B (UVB) radiation in *Daphnia magna*. *Ddc*: aromatic-L-amino-acid decarboxylase; *Hrh1*: histamine H1 receptor; AOX: antioxidants; *Cat*: catalase; *Gst*: glutathione s-transferase; ROS: reactive oxygen species; LPO: lipid peroxidation; lpoROS: lipid peroxidation-associated ROS; MMP: mitochondrial membrane potential; TAG: triglyceride; *Ppar-γ*: peroxisome proliferator-activated receptor gamma coactivator-related protein; FAO: fatty acid oxidation; OXPHOS: oxidative phosphorylation; ATP: adenosine triphosphate; Aifm1: apoptosis-inducing factor 1; *Triap*: TP53-regulated inhibitor of apoptosis 1; *Cacnb1:* voltage-dependent L-type calcium channel subunit beta-1 protein; *Atp2b1*: plasma membrane calcium-transporting ATPase; *CaM*: calmodulin; *EcR-b*: ecdysone receptor B; *Met*: methoprene-tolerant; *Atp1a1*: sodium/potassium-transporting ATPase subunit alpha; *Dnmt1*: DNA (cytosine-5)-methyltransferase 1; 8-OHdG: 8-Oxo-2′-deoxyguanosine; BER: base excision repair; *Ogg1*: oxoguanine glycosylase; NER: nucleotide excision repair; *Xpa*: DNA repair protein complementing XP-A cells; *Ercc1*: DNA excision repair protein ERCC-1; TLS: translesion synthesis; *Rev1*: DNA repair protein REV1; *Rad50*: DNA repair protein RAD50.

D. magna. It has been suggested that ROS-mediated carbonylation of proteins can lead to abnormal Na/K-ATPase, thus affecting osmoregulation.[73] Loss of cellular osmotic pressure may lead to osmotic water flow and accumulation of cellular fluid in crustaceans.[74] In fact, the highest irradiance (0.4 W/m^2) of UVB caused 50% increase in the number of swelled *D. magna* with visible abnormal body fluid accumulation (Figure 1D), whereas lower UVB irradiance did not produce such effects. The swelled daphnids were also found to be unable to maintain normal buoyancy and feed, and appeared to be in an immobilized state. These findings collectively suggest potential loss of osmolarity associated with change in Na/K-ATPase activity and subsequent failure to maintain water balance. Effects of UVB on osmoregulation have never been reported for aquatic crustaceans, but several studies have shown that exposure to other oxidative stressors such as metals can affect osmoregulation in crustaceans (reviewed in ref.[74]). Abnormal body fluid accumulation due to osmotic dysregulation is considered a highly relevant contributor to the observed lethal effects of UVB at the high irradiances tested in this study.

Apical Effects. The histopathological analysis further showed that compared to the controls (Figure 1C, a−e), exposure to the highest irradiance (0.4 W/m^2) of UVB for 2 days led to a number of tissue and organ damage in *D. magna*, such as poor organ compartmentalization (Figure 1C, f), thinner epidermis (Figure 1C, g), lack of embryonic development (Figure 1C, h), abnormal thoracopod development (Figure 1C, i), and malformation of the ovarian structure (Figure 1C, j) compared to the controls. It has been reported that exposure to UVB for 0.5 h (3100 W/m^2) induced cell death-associated delay in embryonic development in the Bristled River Shrimp *Macrobrachium oldersii*.[75] Acute exposure to UVB for 1 h (12 ± 5 W/m^2, total dose: 0.5−1.5 kJ/m^2) caused damage to the skin and muscle cells in earthworms *Amynthas gracilis* and *Metaphire posthuman*.[76] The former species showed cuticle breakdown and epidermis, circular muscle and longitudinal muscle necrosis, whereas the latter displayed epidermal cell necrosis and deformed circular muscle. After 7 days of exposure, 0.2 and 0.4 W/m^2 UVB caused 100% mortality (Figure 1D), whereas a marginal increase in mortality was also observed at 0.05 and 0.1 W/m^2. No mortality was found in the controls or the lowest UVB irradiance (0.008 W/m^2) after 7 days. The median lethal irradiances (LI50s) for 7-day mortality were estimated to be 0.14 W/m^2. An overview of the effect irradiances of different endpoints can be found in Supporting Information −2 (Table S4).

Other Effects. Other types of effects with minor supporting evidence, such as increased transcriptional regulation of negative phototaxis behavior, hormone receptor signaling, and epigenetic regulation, were also considered key events

https://dx.doi.org/10.1021/acs.est.0c03794
Environ. Sci. Technol. XXXX, XXX, XXX−XXX

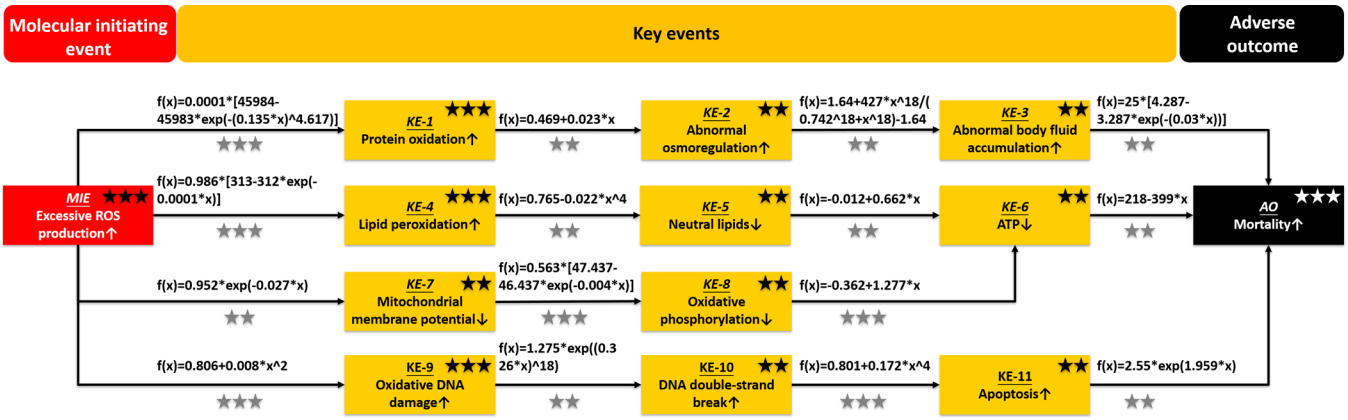

Figure 3. A quantitative adverse outcome pathway (qAOP) network of ultraviolet B (UVB) radiation-mediated lethal effects. Stars indicate weight of evidence: 3 stars = high, 2 stars = moderate, and 1 star = low. Equations are quantitative key event relationship (qKER) models obtained for *Daphnia magna* in the present study. The KER names and quantitative relationships are also summarized in Supporting Information−2, Table S7.

following short-term UVB exposure and discussed in detail in Supporting Information−1.

Toxicity Pathway Assembly. On the basis of the current experimental evidence and relevant UVB-crustacean data extracted from the RAdb (Supporting Information−2, Table S5), a network of toxicity pathways has been proposed to capture the major MoAs of UVB (Figure 2).

AOP Development and Evaluation. Conceptual AOP Network. On the basis of the toxicity pathways, a network of AOPs has been proposed for the lethal effects of UVB and other similarly acting oxidative stressors (Figure 3). In the network, the MIE of excessive ROS production was linked to mortality via four linear AOPs. The names of the KEs are generalized compared to the toxicity pathways to cover a wider range of species and stressors. The four linear AOPs have been submitted to the AOPWiki (AOP #327−330).

Essentiality Assessment of KEs. The essentiality assessment of the KEs (MIE and AO as special KEs) was based on a combination of the current data and existing UVB data extracted from the RAdb (Supporting Information−2, Table S5). Among the 13 KEs proposed in the AOP network (Figure 3), 5 KEs are scored as "high" essentiality as they are supported by direct evidence either from the present study or from the previous data, whereas 8 KEs, such as KE-2 (osmoregulation), KE-8 (oxidative phosphorylation), and KE-10 (DNA DSB), are scored as "moderate", as these are only supported by indirect evidence (i.e., gene expression) from the current study and are not reported for other crustaceans in the published data (Supporting Information −2, Table S6).

WoE Assessment of KERs. A total of 15 KERs are included in the proposed AOPs. The qKERs for UVB-mediated effects were established for *D. magna* using the current data and predefined models (Supporting Information−2, Table S7). The majority of the *D. magna* KER data fit well to at least one of the predefined models (Supporting Information−1, Figure S2), with the exceptions of KER-4 (abnormal body fluid accumulation→mortality), which warrants further data support. Although the qKERs are obtained for *D. magna*, the quantitative understanding of the AOPs is considered weak because (1) the uncertainties of the models still remain high due to the employment of predefined models;[31] (2) the qKER models are established based on one study; and (3) there is still lack of quantitative understanding from other closely related species to confirm the validity of the models. Therefore, more work is needed in modeling approaches as well as in different species to obtain better quantitative understanding of the AOPs.

The biological plausibility of most KERs is considered high (Supporting Information−2, Table S7), as oxidative stress responses, DNA damage responses, mitochondrial functions, and osmoregulation are highly conserved physiological processes and well-documented in aquatic organisms. The relationships between mortality and several KEs, such as decreased ATP, decreased osmoregulation and increased apoptosis; still need to be better established. Data from the present study have also strengthened the empirical support for the KERs. Most of the KERs are considered to have moderate empirical support (Supporting Information−2, Table S7) either from the current study or from other crustacean-UVB studies (Supporting Information −2, Table S5). The KERs associated with ROS-mediated oxidative damage to DNA, protein, and lipids are relatively better investigated in crustaceans and are scored as high for empirical support (Figure 3).

Applicability Domains. The proposed AOP networks are considered applicable to both freshwater and marine planktonic crustaceans with different life stages and genders based on the extracted UVB-crustacean data (Supporting Information−2, Table S5). The taxonomic applicability domain may also be expanded to a wider range of species, as the redox systems, mitochondrial OXPHOS, and DNA repair are highly conserved in the animal kingdom. Data extracted from the NIVA RAdb further showed that in addition to UVB, other oxidative stress-inducing agents, such as metals and organics, are potentially in the stressor applicability domain of the AOP network, as the downstream events of ROS induction are considered similar for multiple oxidative stressors.

■ ASSOCIATED CONTENT

Supporting Information

The Supporting Information is available free of charge at https://pubs.acs.org/doi/10.1021/acs.est.0c03794.

(Supporting Information−1) Full descriptions of materials and methods; additional results and discussion; (Figure S1) spectrum of UVB and UVA; (Figure S2) graphical illustration of NIVA RAdb aided AOP data mining; and (Figure S3) model fitting results (PDF)

https://dx.doi.org/10.1021/acs.est.0c03794
Environ. Sci. Technol. XXXX, XXX, XXX−XXX

(Supporting Information−2) (Table S1) Exposure setup; (Table S2) qPCR primers; (Table S3) UV dosimetry; (Table S4) summary of effect irradiances; (Table S5) data on UVB extracted from NIVA RAdb; (Table S6) summary of KE essentiality assessment; and (Table S7) summary of KER WoE assessment (XLSX)

AUTHOR INFORMATION

Corresponding Authors

You Song − *Norwegian Institute for Water Research (NIVA), N-0349 Oslo, Norway; Centre for Environmental Radioactivity (CERAD), Norwegian University of Life Sciences (NMBU), N-1432 Ås, Norway;* orcid.org/0000-0001-8523-3513; Email: you.song@niva.no

Knut Erik Tollefsen − *Norwegian Institute for Water Research (NIVA), N-0349 Oslo, Norway; Centre for Environmental Radioactivity (CERAD) and Faculty of Environmental Sciences and Natural Resource Management (MINA), Norwegian University of Life Sciences (NMBU), N-1432 Ås, Norway*; Email: knut.erik.tollefsen@niva.no

Authors

Li Xie − *Norwegian Institute for Water Research (NIVA), N-0349 Oslo, Norway; Centre for Environmental Radioactivity (CERAD) and Faculty of Environmental Sciences and Natural Resource Management (MINA), Norwegian University of Life Sciences (NMBU), N-1432 Ås, Norway*

YeonKyeong Lee − *Centre for Environmental Radioactivity (CERAD) and Faculty of Biosciences, Norwegian University of Life Sciences (NMBU), N-1432 Ås, Norway*

Complete contact information is available at: https://pubs.acs.org/10.1021/acs.est.0c03794

Author Contributions

Y.S. conceptualized the study; K.E.T developed the NIVA RAdb and the UV irradiance unit. Y.S., K.E.T., L.X., and Y.L. planned the experimental work; Y.S., L.X., and Y.L. conducted the experimental work; Y.S., L.X., and Y.L. analyzed the experimental data; K.E.T. and Y.S. performed data mining and extraction; Y.S. developed the AOPs and performed qKER modeling; Y.S. drafted the initial manuscript; and K.E.T. ensured the quality of the manuscript. All authors contributed to the manuscript revisions and approved the final submission.

Notes

The authors declare no competing financial interest.

ACKNOWLEDGMENTS

The present work was funded by the Research Council of Norway (RCN) mainly through the Centre of Excellence (CoE) project 223268 "Centre for Environmental Radioactivity (CERAD, www.nmbu.no/en/services/centers/cerad) and partially through project 268294 "Cumulative Risk Assessment of Complex Mixtures and Multiple Stressors (MixRisk, www.niva.no/mixrisk) and project 301397 "Quantitative Adverse Outcome Pathway Assisted Risk Assessment of Mitochondrial Toxicants (RiskAOP, www.niva.no/en/projectweb/riskaop). The development of NIVA RAdb, Y.S., K.E.T. and L.X. were supported by the NIVA Computational Toxicology Program (NCTP, www.niva.no/nctp). The authors would also like to thank Fern Lyne (Newcastle University, UK) for performing the TUNEL assay.

REFERENCES

(1) Ankley, G. T.; Bennett, R. S.; Erickson, R. J.; Hoff, D. J.; Hornung, M. W.; Johnson, R. D.; Mount, D. R.; Nichols, J. W.; Russom, C. L.; Schmieder, P. K.; Serrrano, J. A.; Tietge, J. E.; Villeneuve, D. L. Adverse Outcome Pathways: a conceptual framework to support ecotoxicology research and risk assessment. *Environ. Toxicol. Chem.* **2010**, *29*, 730−741.

(2) Villeneuve, D. L.; Crump, D.; Garcia-Reyero, N.; Hecker, M.; Hutchinson, T. H.; LaLone, C. A.; Landesmann, B.; Lettieri, T.; Munn, S.; Nepelska, M.; Ottinger, M. A.; Vergauwen, L.; Whelan, M. Adverse Outcome Pathway (AOP) development I: Strategies and principles. *Toxicol. Sci.* **2014**, *142*, 312−320.

(3) Villeneuve, D. L.; Crump, D.; Garcia-Reyero, N.; Hecker, M.; Hutchinson, T. H.; LaLone, C. A.; Landesmann, B.; Lettieri, T.; Munn, S.; Nepelska, M.; Ottinger, M. A.; Vergauwen, L.; Whelan, M. Adverse Outcome Pathway development II: Best practices. *Toxicol. Sci.* **2014**, *142*, 321−330.

(4) Becker, R. A.; Ankley, G. T.; Edwards, S. W.; Kennedy, S. W.; Linkov, I.; Meek, B.; Sachana, M.; Segner, H.; Van der Burg, B.; Villeneuve, D. L.; Watanabe, H.; Barton-Maclaren, T. S. Increasing Scientific Confidence in Adverse Outcome Pathways: Application of Tailored Bradford-Hill Considerations for Evaluating Weight of Evidence. *Regul. Toxicol. Pharmacol.* **2015**, *72*, 514−537.

(5) Knapen, D.; Angrish, M. M.; Fortin, M. C.; Katsiadaki, I.; Leonard, M.; Margiotta-Casaluci, L.; Munn, S.; O'Brien, J. M.; Pollesch, N.; Smith, L. C.; Zhang, X. W.; Villeneuve, D. L. Adverse outcome pathway networks I: Development and applications. *Environ. Toxicol. Chem.* **2018**, *37*, 1723−1733.

(6) Villeneuve, D. L.; Angrish, M. M.; Fortin, M. C.; Katsiadaki, I.; Leonard, M.; Margiotta-Casaluci, L.; Munn, S.; O'Brien, J. M.; Pollesch, N. L.; Smith, L. C.; Zhang, X. W.; Knapen, D. Adverse outcome pathway networks II: Network analytics. *Environ. Toxicol. Chem.* **2018**, *37*, 1734−1748.

(7) Tollefsen, K. E.; Scholz, S.; Cronin, M. T.; Edwards, S. W.; de Knecht, J.; Crofton, K.; Garcia-Reyero, N.; Hartung, T.; Worth, A.; Patlewicz, G. Applying Adverse Outcome Pathways (AOPs) to support Integrated Approaches to Testing and Assessment (IATA). *Regul. Toxicol. Pharmacol.* **2014**, *70*, 629−640.

(8) Song, Y.; Xie, L.; Lee, Y.; Brede, D. A.; Lyne, F.; Kassaye, Y.; Thaulow, J.; Caldwell, G.; Salbu, B.; Tollefsen, K. E. Integrative assessment of low-dose gamma radiation effects on *Daphnia magna* reproduction: Toxicity pathway assembly and AOP development. *Sci. Total Environ.* **2020**, *705*, 135912.

(9) Xie, L.; Solhaug, K. A.; Song, Y.; Brede, D. A.; Lind, O. C.; Salbu, B.; Tollefsen, K. E. Modes of action and adverse effects of gamma radiation in an aquatic macrophyte Lemna minor. *Sci. Total Environ.* **2019**, *680*, 23−34.

(10) Hooper, M. J.; Ankley, G. T.; Cristol, D. A.; Maryoung, L. A.; Noyes, P. D.; Pinkerton, K. E. Interactions between chemical and climate stressors: A role for mechanistic toxicology in assessing climate change risks. *Environ. Toxicol. Chem.* **2013**, *32*, 32−48.

(11) Chauhan, V.; Stricklin, D.; Cool, D. The integration of the adverse outcome pathway framework to radiation risk assessment. *Int. J. Radiat. Biol.* **2020**, 1−8.

(12) Chauhan, V.; Sherman, S.; Said, Z.; Yauk, C. L.; Stainforth, R. A case example of a radiation-relevant adverse outcome pathway to lung cancer. *Int. J. Radiat. Biol.* **2019**, 1−17.

(13) Helm, J. S.; Rudel, R. A. Adverse outcome pathways for ionizing radiation and breast cancer involve direct and indirect DNA damage, oxidative stress, inflammation, genomic instability, and interaction with hormonal regulation of the breast. *Arch. Toxicol.* **2020**, *94*, 1511−1549.

(14) Williamson, C. E.; Zepp, R. G.; Lucas, R. M.; Madronich, S.; Austin, A. T.; Ballare, C. L.; Norval, M.; Sulzberger, B.; Bais, A. F.; McKenzie, R. L.; Robinson, S. A.; Hader, D. P.; Paul, N. D.; Bornman, J. F. Solar ultraviolet radiation in a changing climate. *Nat Clim Change* **2014**, *4*, 434−441.

(15) McKenzie, R. L.; Aucamp, P. J.; Bais, A. F.; Bjorn, L. O.; Ilyas, M. Changes in biologically-active ultraviolet radiation reaching the Earth's surface. *Photoch Photobio Sci* **2007**, *6*, 218−231.
(16) Häder, D. P.; Kumar, H. D.; Smith, R. C.; Worrest, R. C. Effects of solar UV radiation on aquatic ecosystems and interactions with climate change. *Photochem. Photobiol. Sci.* **2007**, *6*, 267−285.
(17) Rastogi, R. P.; Richa; Kumar, A.; Tyagi, M. B.; Sinha, R. P. Molecular mechanisms of ultraviolet radiation-induced DNA damage and repair. *J. Nucleic Acids* **2010**, *2010*, 592980.
(18) Cadet, J.; Douki, T.; Ravanat, J. L. Oxidatively generated damage to cellular DNA by UVB and UVA radiation. *Photochem. Photobiol.* **2015**, *91*, 140−155.
(19) Vareschi, E.; Wubben, D. Vertical migration of Daphnia pulex in response to UV radiation. *Int Ver Theor Angew* **2002**, *27*, 3349−3353.
(20) Peng, S.; Liao, H.; Zhou, T.; Peng, S. Effects of UVB radiation on freshwater biota: a meta-analysis. *Global Ecol Biogeogr* **2017**, *26*, 500−510.
(21) Borgeraas, J.; Hessen, D. O. Variations of antioxidant enzymes in *Daphnia* species and populations as related to ambient UV exposure. *Hydrobiologia* **2002**, *477*, 15−30.
(22) Connelly, S. J.; Walling, K.; Wilbert, S. A.; Catlin, D. M.; Monaghan, C. E.; Hlynchuk, S.; Meehl, P. G.; Resch, L. N.; Carrera, J. V.; Bowles, S. M.; Clark, M. D.; Tan, L. T.; Cody, J. A. UV-stressed *Daphnia pulex* increase fitness through uptake of vitamin D3. *PLoS One* **2015**, *10*, No. e0131847.
(23) Miner, B. E.; Kerr, B. Adaptation to variable ultraviolet radiation threats in Alpine *Daphnia* populations. *Integr Comp Biol* **2009**, *49*, E117.
(24) Rautio, M.; Korhola, A. UV-induced pigmentation in subarctic Daphnia. *Limnol Oceanogr* **2002**, *47*, 295−299.
(25) Zellmer, I. D. The effect of solar UVA and UVB on subarctic Daphnia pulicaria in its natural habitat. *Hydrobiologia* **1998**, *379*, 55−62.
(26) OECD, OECD guideline for the testing of chemicals. *In Daphnia magna reproduction test*, OECD: 2012; *211*.
(27) Song, Y.; Salbu, B.; Teien, H. C.; Evensen, Ø.; Lind, O. C.; Rosseland, B. O.; Tollefsen, K. E. Hepatic transcriptional responses in Atlantic salmon (*Salmo salar*) exposed to gamma radiation and depleted uranium singly and in combination. *Sci. Total Environ.* **2016**, *562*, 270−279.
(28) Song, Y.; Rundberget, J. T.; Evenseth, L. M.; Xie, L.; Gomes, T.; Høgasen, T.; Iguchi, T.; Tollefsen, K. E. Whole-organism transcriptomic analysis provides mechanistic insight into the acute toxicity of emamectin benzoate in *Daphnia magna*. *Environ. Sci. Technol.* **2016**, *50*, 11994−12003.
(29) Gomes, T.; Song, Y.; Brede, D. A.; Xie, L.; Gutzkow, K. B.; Salbu, B.; Tollefsen, K. E. Gamma radiation induces dose-dependent oxidative stress and transcriptional alterations in the freshwater crustacean Daphnia magna. *Sci. Total Environ.* **2018**, *628-629*, 206−216.
(30) Jordão, R.; Casas, J.; Fabrias, G.; Campos, B.; Piña, B.; Lemos, M. F.; Soares, A. M.; Tauler, R.; Barata, C. Obesogens beyond Vertebrates: Lipid Perturbation by Tributyltin in the Crustacean Daphnia magna. *Environ. Health Perspect.* **2015**, *123*, 813−819.
(31) Foran, C. M.; Rycroft, T.; Keisler, J.; Perkins, E. J.; Linkov, I.; Garcia-Reyero, N. A modular approach for assembly of quantitative adverse outcome pathways. *ALTEX* **2019**, *36*, 353−3620.
(32) Davis, J. A.; Gift, J. S.; Zhao, Q. J. Introduction to benchmark dose methods and U.S. EPA's benchmark dose software (BMDS) version 2.1.1. *Toxicol Appl Pharm* **2011**, *254*, 181−191.
(33) OECD, Users' Handbook supplement to the guidance document for developing and assessing Adverse Outcome Pathways. *In OECD Series on Adverse Outcome Pathways, No. 1*, OECD Publishing: Paris, 2018.
(34) Birben, E.; Sahiner, U. M.; Sackesen, C.; Erzurum, S.; Kalayci, O. Oxidative stress and antioxidant defense. *World Allergy Organ J* **2012**, *5*, 9−19.
(35) Borgeraas, J.; Hessen, D. O. UV-B induced mortality and antioxidant enzyme activities in Daphnia magna at different oxygen concentrations and temperatures. *J Plankton Res* **2000**, *22*, 1167−1183.
(36) Oexle, S.; Jansen, M.; Pauwels, K.; Sommaruga, R.; De Meester, L.; Stoks, R. Rapid evolution of antioxidant defense in a natural population of *Daphnia magna*. *J Evol Biol* **2016**, *29*, 1328−1337.
(37) Won, E. J.; Lee, Y.; Han, J.; Hwang, U. K.; Shin, K. H.; Park, H. G.; Lee, J. S. Effects of UV radiation on hatching, lipid peroxidation, and fatty acid composition in the copepod Paracyclopina nana. *Comp Biochem Phys C* **2014**, *165*, 60−66.
(38) Kim, B. M.; Rhee, J. S.; Lee, K. W.; Kim, M. J.; Shin, K. H.; Lee, S. J.; Lee, Y. M.; Lee, J. S. UV-B radiation-induced oxidative stress and p38 signaling pathway involvement in the benthic copepod Tigriopus japonicus. *Comp Biochem Physiol C Toxicol Pharmacol* **2015**, *167*, 15−23.
(39) Cadet, J.; Sage, E.; Douki, T. Ultraviolet radiation-mediated damage to cellular DNA. *Mutat. Res.* **2005**, *571*, 3−17.
(40) Douki, T.; Perdiz, D.; Grof, P.; Kuluncsics, Z.; Moustacchi, E.; Cadet, J.; Sage, E. Oxidation of guanine in cellular DNA by solar UV radiation: Biological role. *Photochem. Photobiol.* **1999**, *70*, 184−190.
(41) Waters, L. S.; Walker, G. C. The critical mutagenic translesion DNA polymerase Rev1 is highly expressed during G₂/M phase rather than S phase. *Pro. Nat. Aca.Sci.* **2006**, *103*, 8971−8976.
(42) Rhee, J. S.; Kim, B. M.; Choi, B. S.; Lee, J. S. Expression pattern analysis of DNA repair-related and DNA damage response genes revealed by 55K oligomicroarray upon UV-B irradiation in the intertidal copepod, Tigriopus japonicus. *Comp Biochem Physiol C Toxicol Pharmacol* **2012**, *155*, 359−368.
(43) Connelly, S. J.; Moeller, R. E.; Sanchez, G.; Mitchell, D. L. Temperature effects on survival and DNA repair in four freshwater cladoceran *Daphnia* species exposed to UV radiation. *Photochem. Photobiol.* **2009**, *85*, 144−152.
(44) Kim, B.-M.; Rhee, J.-S.; Seo, J. S.; Kim, I.-C.; Lee, Y.-M.; Lee, J.-S. 8-Oxoguanine DNA glycosylase 1 (OGG1) from the copepod Tigriopus japonicus: Molecular characterization and its expression in response to UV-B and heavy metals. *Comp. Biochem. Physiol., Part C: Toxicol. Pharmacol.* **2012**, *155*, 290−299.
(45) Krejci, L.; Chen, L.; Komen, S. V.; Sung, P.; Tomkinson, A., Mending the Break: Two DNA Double-Strand Break Repair Machines in Eukaryotes. *In Progress in Nucleic Acid Research and Molecular Biology*, Academic Press: 2003; *74*, 159−201, DOI: 10.1016/S0079-6603(03)01013-4.
(46) Kaina, B. DNA damage-triggered apoptosis: critical role of DNA repair, double-strand breaks, cell proliferation and signaling. *Biochem. Pharmacol.* **2003**, *66*, 1547−1554.
(47) Menze, M. A.; Fortner, G.; Nag, S.; Hand, S. C. Mechanisms of apoptosis in Crustacea: what conditions induce versus suppress cell death? *Apoptosis* **2010**, *15*, 293−312.
(48) Susin, S. A.; Lorenzo, H. K.; Zamzami, N.; Marzo, I.; Snow, B. E.; Brothers, G. M.; Mangion, J.; Jacotot, E.; Costantini, P.; Loeffler, M.; Larochette, N.; Goodlett, D. R.; Aebersold, R.; Siderovski, D. P.; Penninger, J. M.; Kroemer, G. Molecular characterization of mitochondrial apoptosis-inducing factor. *Nature* **1999**, *397*, 441−446.
(49) Adams, C.; Cazzanelli, G.; Rasul, S.; Hitchinson, B.; Hu, Y.; Coombes, R. C.; Raguz, S.; Yagüe, E. Apoptosis inhibitor TRIAP1 is a novel effector of drug resistance. *Oncol. Rep.* **2015**, *34*, 415−422.
(50) Hollmann, G.; Ferreira, G. d. J.; Geihs, M. A.; Vargas, M. A.; Nery, L. E. M.; Leitão, Á.; Linden, R.; Allodi, S. Antioxidant activity stimulated by ultraviolet radiation in the nervous system of a crustacean. *Aquat. Toxicol.* **2015**, *160*, 151−162.
(51) Schramm, H.; Jaramillo, M. L.; Quadros, T. d.; Zeni, E. C.; Müller, Y. M. R.; Ammar, D.; Nazari, E. M. Effect of UVB radiation exposure in the expression of genes and proteins related to apoptosis in freshwater prawn embryos. *Aquat. Toxicol.* **2017**, *191*, 25−33.
(52) Ayala, A.; Munoz, M. F.; Arguelles, S. Lipid peroxidation: production, metabolism, and signaling mechanisms of malondialde-

https://dx.doi.org/10.1021/acs.est.0c03794
Environ. Sci. Technol. XXXX, XXX, XXX−XXX

hyde and 4-hydroxy-2-nonenal. *Oxid. Med. Cell. Longevity* **2014**, *2014*, 360438.
(53) Walther, T. C.; Farese, R. V. J. Lipid Droplets and Cellular Lipid Metabolism. *Annu. Rev. Biochem.* **2012**, *81*, 687−714.
(54) Casares, D.; Escribá, P. V.; Rosselló, C. A. Membrane Lipid Composition: Effect on Membrane and Organelle Structure, Function and Compartmentalization and Therapeutic Avenues. *Int. J. Mol. Sci.* **2019**, *20*, 2167.
(55) Ribeiro, F.; Ferreira, N. C. G.; Ferreira, A.; Soares, A. M. V. M.; Loureiro, S. Is ultraviolet radiation a synergistic stressor in combined exposures? The case study of Daphnia magna exposure to UV and carbendazim. *Aquat. Toxicol.* **2011**, *102*, 114−122.
(56) Houten, S. M.; Violante, S.; Ventura, F. V.; Wanders, R. J. A. The Biochemistry and Physiology of Mitochondrial Fatty Acid β-Oxidation and Its Genetic Disorders. *Annu. Rev. Physiol.* **2016**, *78*, 23−44.
(57) Lee, C.-H.; Olson, P.; Evans, R. M. Minireview: Lipid Metabolism, Metabolic Diseases, and Peroxisome Proliferator-Activated Receptors. *Endocrinology* **2003**, *144*, 2201−2207.
(58) Hosseini, M.; Dousset, L.; Mahfouf, W.; Serrano-Sanchez, M.; Redonnet-Vernhet, I.; Mesli, S.; Kasraian, Z.; Obre, E.; Bonneu, M.; Claverol, S.; Vlaski, M.; Ivanovic, Z.; Rachidi, W.; Douki, T.; Taieb, A.; Bouzier-Sore, A. K.; Rossignol, R.; Rezvani, H. R. Energy Metabolism Rewiring Precedes UVB-Induced Primary Skin Tumor Formation. *Cell Rep.* **2018**, *23*, 3621−3634.
(59) Bonora, M.; Patergnani, S.; Rimessi, A.; De Marchi, E.; Suski, J. M.; Bononi, A.; Giorgi, C.; Marchi, S.; Missiroli, S.; Poletti, F.; Wieckowski, M. R.; Pinton, P. ATP synthesis and storage. *Purinergic Signal* **2012**, *8*, 343−357.
(60) Hardie, D. G. AMP-activated protein kinase—an energy sensor that regulates all aspects of cell function. *Gene Dev* **2011**, *25*, 1895−1908.
(61) de Quadros, T.; Schramm, H.; Zeni, E. C.; Simioni, C.; Allodi, S.; Müller, Y. M. R.; Ammar, D.; Nazari, E. M. Developmental effects of exposure to ultraviolet B radiation on the freshwater prawn Macrobrachium olfersi: Mitochondria as a target of environmental UVB radiation. *Ecotox Environ Safe* **2016**, *132*, 279−287.
(62) Bruce, J. Plasma membrane calcium pump regulation by metabolic stress. *World J Biol Chem* **2010**, *1*, 221−228.
(63) Gadsby, D. C. Ion channels versus ion pumps: the principal difference, in principle. *Nat Rev Mol Cell Biol* **2009**, *10*, 344−352.
(64) Eguchi, Y.; Shimizu, S.; Tsujimoto, Y. Intracellular ATP levels determine cell death fate by apoptosis or necrosis. *Cancer Res.* **1997**, *57*, 1835−1840.
(65) Kiselyov, K.; Muallem, S. ROS and intracellular ion channels. *Cell Calcium* **2016**, *60*, 108−114.
(66) Kourie, J. I. Interaction of reactive oxygen species with ion transport mechanisms. *Am J Physiol* **1998**, *275*, C1−C24.
(67) Chin, D.; Means, A. R. Calmodulin: a prototypical calcium sensor. *Trends in Cell Bio.* **2000**, *10*, 322−328.
(68) Snutch, T. P., Voltage-Gated Calcium Channels. In *Encyclopedia of Neuroscience*, Squire, L. R.; Academic Press: Oxford, 2009; 427−441.
(69) Wu, Q.; Guo, D.; Bi, H.; Wang, D.; Du, Y. UVB irradiation-induced dysregulation of plasma membrane calcium ATPase1 and intracellular calcium homeostasis in human lens epithelial cells. *Mol. Cell. Biochem.* **2013**, *382*, 263−272.
(70) Duchen, M. R. Mitochondria and calcium: from cell signalling to cell death. *J Physiol* **2000**, *529*, 57−68.
(71) Orrenius, S.; Zhivotovsky, B.; Nicotera, P. Regulation of cell death: the calcium-apoptosis link. *Nat Rev Mol Cell Biol* **2003**, *4*, 552−565.
(72) Li, Z.; Langhans, S. A. Transcriptional regulators of Na K-ATPase subunits. *Front. in Cell and Develop. Bio.* **2015**, *3*, 66.
(73) Shah, P. T.; Martin, R.; Yan, Y.; Shapiro, J. I.; Liu, J. Carbonylation Modification Regulates Na/K-ATPase Signaling and Salt Sensitivity: A Review and a Hypothesis. *Front Physiol* **2016**, *7*, 256.
(74) Péqueux, A. Osmotic Regulation in Crustaceans. *J Crustacean Biol* **1995**, *15*, 1−60.
(75) Müller, Y. M. R.; Quadros, T. d.; Schramm, H.; Weiss, V. M. C.; Zeni, E. C.; Nazari, E. M.; Ammar, D., Biometrical and morphological analyses of Macrobrachium olfersii (Wiegmann, 1836) (Crustacea, Decapoda, Palaemonidae) embryos exposed to UVA and UVB radiation. *Nauplius* 2018, *26*, DOI: 10.1590/2358-2936e2018013.
(76) Chuang, S.-C.; Lai, W.-S.; Chen, J.-H. Influence of ultraviolet radiation on selected physiological responses of earthworms. *J Exp Biol* **2006**, *209*, 4304−4312.

https://dx.doi.org/10.1021/acs.est.0c03794
Environ. Sci. Technol. XXXX, XXX, XXX−XXX